Macromolecules

pubs.acs.org/Macromolecules
Article

Correlation Between Segmental Order Parameter and Entanglement Length in a Monodisperse Comb Polymer

Farhad Shahsavan,* Jonas Keller, Manfred Wilhelm, and Kay Saalwächter*

Cite This: *Macromolecules* 2024, 57, 11030−11041

ABSTRACT: The motion of a polymer chain within a hypothetical confining tube gives rise to a segmental order parameter S_b. This parameter is assessed via multiple-quantum (MQ) NMR experiments, providing a valuable molecule-level rheological observable. In both polymer networks and entangled melts, the order parameter is proportional to the inverse of the number of segments between two covalent cross-links or physical entanglements. In entangled polymer networks, the entanglements have usually been considered as additional but temporary cross-links and the contribution of the physical and chemical constraints are assumed additive. Recent computer simulation results challenged this assumption for lowly cross-linked polymer networks; instead, S_b was shown to scale with $(N_e N_c)^{-1/2}$, N_c and N_e being the number of segments between cross-links and entanglements, respectively [Lang, M.; Sommer, J.-U., *Phys. Rev. Lett.* **2010**, *104*, 177801]. An experimental confirmation remains elusive due to challenges in distinguishing the contributions of entanglements and cross-links, as well as the long averaging time scales involved. In this study, we assess this correlation by examining chain dynamics in a monodisperse polyisoprene comb, utilized as a model system. To model chain dynamics in this system, the dynamic tube dilation model, originally designed for predicting the rheological behavior of star and branched polymers, has been modified to facilitate its application in the analysis of MQ NMR signals. We also address some of its shortcomings.

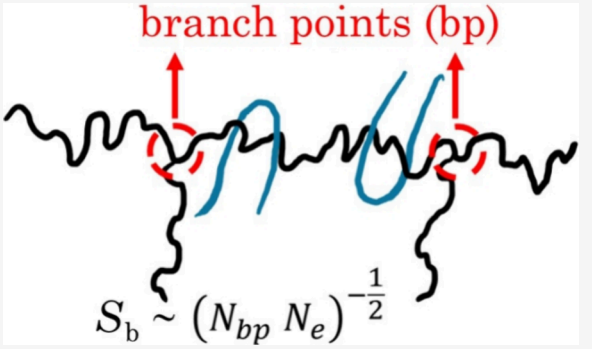

INTRODUCTION

The tube model provides a theoretical framework for characterizing the dynamics of polymer chains in both polymer melts and networks.[1−3] Apart from its use in understanding and predicting the mechanical properties, an implementation for the analysis of time-domain proton solid-state NMR data offers a powerful means to investigate motions involving numerous segments, even up to the scale of whole chains in terms of characteristic time scales and the segmental order parameter, which are in turn related to the macroscopic properties of polymeric systems.[4−6] This capability makes solid-state NMR a valuable tool to probe the segmental dynamics occurring within the constrained tube formed by neighboring chains or cross-links in polymer melts and networks, respectively.

Time-domain ^{1}H multiple-quantum NMR (MQ NMR) technique is a quantitative approach relying on the orientation-dependent intrasegmental proton magnetic dipole−dipole coupling, that probes the segmental dynamics in terms of the orientation autocorrelation function (OACF) of the second Legendre polynomial, denoted as $C(t) = 5 \langle P_2(\cos\theta(t+\tau)) P_2(\cos\theta(\tau))\rangle_\tau$ where θ represents the instantaneous orientation of the segmental vector with respect to the external magnetic field vector. The OACF describes the probability of finding segments remain in the same orientation after passing a specific time t. The OACF has been used to quantify the chain dynamics in monodisperse polymer melts,[5−9] transient networks[10,11] and even in a partially cross-linked network.[12] In the case of polymer melts, the constraint release and contour length fluctuations corrections to the tube model predictions could be confirmed.

In polymer networks, an averaged residual magnetic dipolar coupling (D_{res}) arises from the fast but anisotropic dynamics of polymer chains arising from spatial constraints (entanglements and cross-links).[4] The quantity D_{res} is proportional to the segmental order parameter $S_b \sim N_{el}^{-1}$, and accordingly to the inverse of constrained chain length N_{el}.[13] D_{res} and its distribution have been comprehensively probed for assessment of the network structure in well-developed elastomers[14−17] and hydrogels.[18] In entangled polymer networks, entanglements play an active role in the elasticity. To relate the NMR data to the structure, entanglements were assumed as additional cross-

Received: August 23, 2024
Revised: October 30, 2024
Accepted: November 14, 2024
Published: November 25, 2024

https://doi.org/10.1021/acs.macromol.4c02015
Macromolecules 2024, 57, 11030−11041

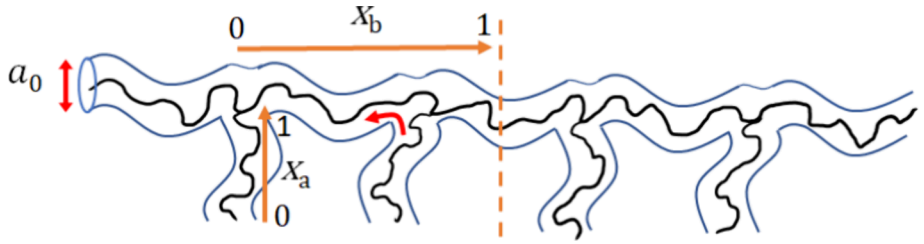

Figure 1. Schematic representation of a polymer comb, defining the segmental curvilinear coordinate, which is 0 at free ends of arms and at the first branch point in the backbone. Center of the backbone is located at $x_b = 1$.

links and accordingly the contributions of physical and chemical constraints were assumed to be additive.[19] Thus, considering the inverse relation between subchain length and constraint density, the effective elastic chain length N_{el} may be written as follows:

$$N_{el}^{-1} = N_c^{-1} + N_e^{-1} \approx N_e^{-1} \text{ for } N_c \gg N_e \quad (1)$$

Here, N_c and N_e are the average chain length between two chemical strands and the entanglement length, respectively. According to the above equation in lowly cross-linked system, the order parameter correlates with the inverse of entanglement length.

However, it was shown theoretically by Lang and Sommer[1] that in entangled networks, the entanglement contribution is not simply additive in the apparent cross-link density reflected by $D_{res} \sim S_b$. They showed that the long-time plateau value of segmental order parameter scales as $S_b \sim (N_c N_e)^{-1/2}$ rather than $\sim(1/N_e + 1/N_c)$, which is the result of the longitudinal segmental fluctuations along the confining tube (back-and-forth local reptation) for entangled networks, confirmed by computer simulations. For an NMR-based experimental investigation of entangled polymer networks, it is necessary to be in fast-motion limit, i.e., the subchain between two cross-links should sweep out its full conformational space within the experimental time scale (consider that in entangled networks, the length between two cross-links is at least two times longer than the entanglement length). Accordingly, lowly cross-linked polymer networks need to be probed at very high temperatures, which is often above the degradation temperature of many common rubbers. The study of swollen low-cross-linked polymer networks in a good solvent[20] can be an alternative approach though in this case the data suffers from non isochronal condition due to the dilution.

As a pragmatic alternative, one can investigate the proportionality of the segmental order parameter with entanglement length in a system analogous to a lowly cross-linked polymer network. In this study, we employed a polyisoprene comb polymer, where the attachment points of the arms serve as cross-links. The distance between arms is approximately twice the entanglement length (N_e), making it a suitable analog for probing the segmental order parameter.

The chain dynamics of this comb polymer system can be predicted using dynamic tube dilation (DTD) theory. In this theory, the effect of relaxed segments is considered analogous to solvent molecules, which dilute the entanglements and thus dilate the tube around the arms and backbone. For a monodisperse comb polymer, the population of relaxed segments is treated as a position-dependent parameter, depending solely on the location of a specific segment in the arms or backbone and independent of time. In contrast, to study polydisperse branched polymers or blends of linear and star polymers, a time-dependent fraction of relaxed segments is used in the improved hierarchical relaxation model.[21−24]

In this work, the polyisoprene comb polymer serves as an analogous model to probe the segmental order parameter in lowly cross-linked, branched systems. We explored both possible relationships between the segmental order parameter and entanglement length within the framework of the DTD model. Notably, we experimentally confirmed for the first time that the segmental order parameter scales as $S_b \sim (N_e)^{-1/2}$. The findings and methodology developed in this work can pave the way for the application of the MQ NMR technique to determine structural parameters (such as arm and backbone molecular weight and the number of branches) in branched polymers. The significance of this work extends beyond studying polymer chain dynamics within the framework of the tube/reptation model. We developed a method to evaluate the position-dependent dynamics of polymer segments using MQ NMR technique, applicable to systems with similar relaxation behavior. This method offers the opportunity to directly extract the relaxation time profile of confined polymer chains in polymer (nano)composites via ^{1}H MQ NMR, establishing it as a powerful "molecular rheology" tool in polymer science.

THEORETICAL BACKGROUND

Relaxation Spectrum of Comb Polymers. In linear polymers, the polymer motions are restricted to diffusion along the tube formed by the neighboring chains. In a long-branched polymer, the reptation along the tube is not simply linear. In this material class, a hierarchical relaxation is assumed for the segments in arms and backbone.[25,26] The spectrum of the relaxation times is governed not only by topological parameters of the comb polymer but also by the population of already relaxed segments in the surroundings. Segments that are considered relaxed (at a given time t) have reached their respective, position-dependent terminal time τ_i needed for effectively isotropic motion, thus pragmatically calculating the individual contribution to the relaxed population as their residual correlation $\sim e^{-t/\tau_i}$. To consider the dilution effect of relaxed segments, which is similar to constraint release, DTD theory assumes a dilated confining tube.[27−29]

According to the DTD model, a relaxed segment is considered an effective athermal solvent, and by its dilution effect, the remaining segments move in a dilated tube. In arms, the chains relax via arm retraction process (Rouse motion) whereas in the backbone, the relaxation is governed by two motions including contour length fluctuation and reptation motion. Reptation occurs at longer times when it becomes the dominant process.[30,31] The full spectrum of arm and backbone relaxation in a comb polymer can be found in ref 30.

https://doi.org/10.1021/acs.macromol.4c02015
Macromolecules 2024, 57, 11030−11041

The effective modulus of a diluted entanglement network can be written as follows:

$$G(\Phi) = G_0\Phi^{\beta} \tag{2}$$

Here, β is a scaling exponent (see below) and Φ the fraction of unrelaxed segments. It can be defined at any relaxation time $\tau(x)$, as a function of the segmental curvilinear dimensionless coordinate (see Figure 1): $\Phi(x) = 1 - x$. Thus, for the stress relaxation modulus, a general expression can be written:

$$G(t) = \int_0^1 \frac{\partial G[\Phi(x)]}{\partial x}\exp\left[-\frac{t}{\tau(x)}\right]\mathrm{d}x \tag{3}$$

This expression assumes that the effective modulus at time t depends on the fraction of the unrelaxed tube. The above equation can be divided into two contributions for a comb polymer:[32,33]

$$G(t) = G_0\beta\left\{\int_0^1 {\varphi_{bb}}^{\beta}(1 - x_{bb})^{\beta-1}\exp\left[\frac{-t}{\tau_{bb}(x_{bb})}\right]\mathrm{d}x_{bb} + \int_0^1 \varphi_a(1 - \varphi_a x_a)^{\beta-1}\exp\left[\frac{-t}{\tau_a(x_a)}\right]\mathrm{d}x_a\right\} \tag{4}$$

The equation's first term represents the backbone's contribution (subscript "bb") and the second term expresses the arms' contribution ("a") to stress relaxation. Equation 4 has usually been written in terms of $\alpha = \beta - 1$ for simplicity, where α is the dilution exponent that can be 1 or 4/3.[34,35]

The stress relaxation for the different regimes beyond Rouse can be found as follows:[30,31]

Arm retraction:

$$G_a = G_N(1 + \alpha)\varphi_a\int_0^1 (1 - \varphi_a x_a)^{\alpha}\exp\left[-\frac{t}{\tau_a(x_a)}\right]\mathrm{d}x_a \tag{5}$$

Contour length fluctuation (in backbone):

$$G_{bb} = G_N(1 + \alpha){\varphi_{bb}}^{1+\alpha}\int_0^{x_d}(1 - x_{bb})^{\alpha} \times \exp\left[-\frac{t}{\tau_{bb}(x_{bb})}\right]\mathrm{d}x_{bb} \tag{6}$$

Reptation:

$$G_{rept} = G_N[\varphi_{bb}(1 - x_d)]^{1+\alpha}\sum_{q=\mathrm{odd}}\frac{8}{q^2\pi^2}\exp\left[-\frac{q^2 t}{\tau_d(x_d)}\right] \tag{7}$$

We refrain from reproducing the rather lengthy expressions for the relaxation times $\tau_a(x_a)$, $\tau_{bb}(x_{bb})$ and $\tau_d(x_d)$, which can be found in the literature.[25,30,31] A concise summary is given in ref 36. The complex dependencies of $\tau_a(x_a)$, $\tau_{bb}(x_{bb})$ on the dimensionless coordinates $x_{a,bb}$ are derived by smoothly crossing over from an early rouse-like relaxation (early arm/backbone relaxation time) to slower "activated" relaxations (late arm/backbone relaxation time). The outermost part of the arm or backbone follows constrained Rouse motion, whereas the retraction process of the intermediate and innermost segments is governed by diffusion over a barrier $U_{eff}(x_{a,bb})$ of entropic origin. Apart from the explicit $x_{a,bb,d}$ dependencies and the implicit dependence on the dilution exponent α, these parameters also depend on relevant material parameters, specifically the number of entanglements $Z_{a,bb} = M_{a,bb}/M_e$, the entanglement time τ_e and the arm/backbone volume fractions $\varphi_{a,bb}$. Upon fitting, M_e and τ_e will be considered free parameters. Furthermore, τ_{bb} and τ_d depend on an additional empirical dimensionless parameter p, the inverse of which is the fraction of the (dilated) tube diameter by which a fully relaxed arm can hop. Even though this quantity may be considered time-dependent (accounting for the ongoing tube dilation effect), it seems that most works considered it as a constant "fudge parameter". Unless discussed otherwise, its value is taken to be $1/\sqrt{12}$.[30] Other recent studies stated that it can be as low as $1/\sqrt{40}$,[24] yet we will show that variations in this range have minor effects on the outcome. A possible time dependence of the fraction of unrelaxed segments to account for the ongoing tube dilation will be considered in a separate section.

We are fully aware that the DTD model predictions discussed herein feature good precision for monodisperse branched polymers but do not quite represent the state of the art in modeling the rheological response of polydisperse systems. Alternative approaches exist that provide more quantitative modeling and predictions,[37−39] but are numerically even more complex and challenging with regards to their implementation. In our hands, the given approach enabled a direct implementation for the prediction of NMR observables for the first time.

MQ NMR Interpretation of the DTD Hypothesis. Proton multiple-quantum (MQ) NMR is a sensitive method for measuring residual dipolar coupling, particularly in polymer melts and networks. As explained above, the presence of entanglements and cross-links as topological constraints in a polymer structure causes anisotropic motion of chains that leads to a residual dipolar coupling. In the fast-motion limit where the segments move fast enough to occupy all the possible conformations on the time scale of hundreds of microseconds up to a few milliseconds, D_{res} reflects the local dynamic order parameter S_b via the following equation:

$$S_b = \langle P_2(\cos\theta)\rangle = k\frac{D_{res}}{D_{stat}} = \frac{3}{5N}\frac{r^2}{\langle r_0^2\rangle} \tag{8}$$

D_{stat} is the static dipolar coupling constant, k is a constant that corrects static dipolar coupling for very fast intrasegmental motions, N is the number of Kuhn monomers between two topological constraints, and the last term quantifies the state of stretching of the end-to-end distance r of the subchain as compared to its unperturbed averaged value in the molten state (which may change upon (de)swelling and macroscopic deformation, both irrelevant in the present work). Implicit to this treatment is that in fitting the MQ NMR data, the Rouse regime is neglected, as experimentally relevant times always exceed the entanglement time τ_e. We note that the subscript "b" in the order parameter S_b of Kuhn segments originally also referred polymer backbone (as the reference direction for the orientation angle relative to the end-to-end vector); for the branched systems at hand, it also stands for segments in arms.

By phase cycling, two signals, I_{ref} and I_{DQ}, are recorded as a function of double-quantum (DQ) evolution time, i.e., the duration of the applied pulse sequence.[4] The DQ intensity I_{DQ} contains signals from coupled protons that are part of the chains with anisotropic motions, whereas the multiple-quantum (MQ) sum signal $I_{\Sigma MQ} = I_{ref} + I_{DQ}$ (normalized to unity at $\tau_{DQ} = 0$) reflects the transverse (T_2) relaxation of all

https://doi.org/10.1021/acs.macromol.4c02015
Macromolecules 2024, 57, 11030−11041

protons, including anisotropic moieties (coupled protons) and isotropic moieties. The amount of isotropically mobile polymer-chain defects is usually reflected by a mono- or biexponential long-time tail of $I_{\Sigma MQ}$.

According to the spin-pair-based quantum-mechanical treatment in combination with Andersson-Weiss (AW) approximation,[40] the MQ NMR signal functions can be written:

$$I_{DQ} = \sinh\langle\phi_1\phi_2\rangle e^{-\langle\phi_1^2\rangle} \tag{9}$$

$$I_{ref} = \cosh\langle\phi_1\phi_2\rangle e^{-\langle\phi_1^2\rangle} \tag{10}$$

$$I_{\Sigma MQ} = e^{\langle\phi_1\phi_2\rangle} e^{-\langle\phi_1^2\rangle} \tag{11}$$

In the second step of the AW approximation, the time and ensemble averages of the spin-evolution phases ϕ_i are evolved as simple time integrals of the orientation autocorrelation function (OACF):[41,42]

$$\langle\phi_1(0, \tau)^2\rangle = \frac{4}{9} M_{2eff} \times 2 \int_0^\tau (\tau - t')C(t')dt' \tag{12}$$

$$\langle\phi_1(0, \tau)\phi_2(\tau, 2\tau)\rangle = \frac{4}{9} M_{2eff}\left[\int_0^\tau t'C(t')dt' + \int_\tau^{2\tau} (2\tau - t')C(t')dt'\right] \tag{13}$$

$C(t)$ represents the probability of finding a segment in the same orientation after a specific time and $M_{2eff} = (9/20)(D_{stat}/k)$ is the effective dipolar second moment related to a Kuhn segment. In the fitting functions derived below, M_{2eff} will be absorbed into $C(t) \sim S_b^2$, leaving D_{res} as a fitting parameter according to eq 8.

The above considerations are valid for any MQ NMR experiment featuring a pure DQ average Hamiltonian (providing clean dipolar spin evolution into higher even-order coherences), such as our most-used pulse sequence developed by Baum and Pines.[4,43] Details of the implementation, such as using short repetitive pulse sequence cycles or cycle time incrementation to realize a specific τ_{DQ}, were shown to have a minor effect on the calculated signal functions.[7] For other types of NMR experiments, a nontrivial effect of interchain dipole−dipole couplings on polymer dynamics observables has been reported.[44,45] However, in our hands, MQ NMR provides a faithful measure of the shape of the segmental OACF, with the intercouplings merely leading to an adjustment of the absolute value of M_{2eff} or D_{res}.[9]

MQ NMR can thus probe the hierarchy of the relaxation times in terms of the OACF. According to the DTD hypothesis, tube dilation results from the relaxation of segments. Thus, an explicit relation between the OACF and the fraction of unrelaxed segments is required. According to eq 8, which is valid for linear polymer melts as well as networks, the order parameter correlates with the inverse entanglement length. Consequently, we can write

$$C(t) \approx S_b(t)^2 \sim N_e(t)^{-2} \sim \Phi(t)^{2\alpha} \tag{14}$$

On the other hand, Lang and Sommer[1] have shown that in lowly cross-linked systems with many entanglements between permanent constraints, the order parameter scales with $S_b \sim (NN_e)^{-0.5}$, where N is the number of segments between two permanent strands. The inner part of the polymer comb backbone states between two branch points temporarily immobilized by the long arms. Due to the described analogy, the OACF can thus be written in terms of the entanglement length as

$$C(t) \approx S_b(t)^2 \sim N_e(t)^{-1} \sim \Phi(t)^{\alpha} \tag{15}$$

Since we are using the DTD model to describe MQ NMR signals for the first time in the current work, both exponents in eqs 14 and 15 are considered for analyzing the data. From now on, the generalized and a-priori unknown OACF-related dilution exponent is denoted by γ to avoid any misunderstanding:

$$C(t) \sim \Phi(t)^{\gamma} \tag{16}$$

Quantitatively, in analogy to the rheology theory, a characteristic OACF can be defined for every segment based on the DTD effect discussed so far and its position-dependent characteristic relaxation time:

$$C(t, x_{a,bb}) = S_{b,0}{}^2 \Phi(t)^{\gamma} \exp\left[-\frac{t}{\tau_{a,bb}(x_{a,bb})}\right] \tag{17}$$

Here, $S_{b,0}$ is defined as the order parameter corresponding to the entanglement-related rubbery plateau of the OACF (that would arise if constraints were fixed). As mentioned in the context of eqs 8, 12, 13, we remind that the relevant fitting parameter will be the entanglement-related residual dipolar coupling $D_{res,0} \sim S_{b,0}$. Again in analogy to the rheological modeling, the fraction of relaxed segments is now taken to be equal to the dimensionless segmental coordinate at any time according to the suggested interpretation of the DTD assumption for monodisperse comb (and H) polymers.[30,32] In this interpretation, it is assumed that when a segment relaxes, all segments with shorter relaxation times have already relaxed. Thus, the fraction of relaxed segments is defined only based on the segmental coordinate (e.g., for a segment in an arm at position x_a, the fraction of relaxed segment is $\varphi_a x_a$) at any time. Obviously, this is only valid at times longer than the corresponding relaxation time. In rheology, although fits reproduce the tube model parameters really well, this assumption leads to an overestimation of the arms' contribution in the storage modulus at short times, while in the MQ NMR, it causes physically meaningless correlation functions for arms and backbone. Both issues and possible solutions are discussed below.

The normalized OACF for arm segments and backbone segments can thus be written, respectively, as

$$C(t, x_a) = S_{b,0}{}^2(1 - \varphi_a x_a)^{\gamma} \exp\left[-\frac{t}{\tau_a(x_a)}\right] \tag{18}$$

$$C(t, x_{bb}) = S_{b,0}{}^2[\varphi_{bb}(1 - x_{bb})]^{\gamma} \exp\left[-\frac{t}{\tau_{bb}(x_{bb})}\right] \tag{19}$$

Using the AW approximation, the signal functions for a simple exponential decay read as follows:[7]

https://doi.org/10.1021/acs.macromol.4c02015
Macromolecules 2024, 57, 11030−11041

$$I_{DQ}^{a,bb}(\tau_{DQ}, \tau_p, D_{res}(x_{a,bb})) = \exp\left[-0.4D_{res}(x_{a,bb})^2\tau_{a,bb}{}^2\left(e^{-\tau_{DQ}/\tau_{a,bb}} + \frac{\tau_{DQ}}{\tau_{a,bb}} - 1\right)\right] \times \sinh\{0.2D_{res}(x_{a,bb})^2\tau_{a,bb}{}^2(e^{-2\tau_{DQ}/\tau_{a,bb}} - 2e^{-\tau_{DQ}/\tau_{a,bb}} + 1)\} \quad (20)$$

$$I_{\Sigma MQ}^{a,bb}(\tau_{DQ}, \tau_p, D_{res}(x_{a,bb})) = \exp\left\{-0.2D_{res}(x_{a,bb})^2\tau_{a,bb}{}^2\left[4e^{-\tau_{DQ}/\tau_{a,bb}} - e^{-2\tau_{DQ}/\tau_{a,bb}} + \frac{2\tau_{DQ}}{\tau_{a,bb}} - 3\right]\right\} \quad (21)$$

Here, $\tau_{a,bb}$ is the relaxation time of a single segment corresponding to the relevant process (either arm retraction or backbone CLF processes, which also define the D_{res} function). $D_{res}(x_{a,bb})^2$ are the prefactors of eqs 18 and 19 in terms of D_{res}, i.e., $D_{res,0}{}^2(1 - \varphi_a x_a)^\gamma$ or $D_{res,0}{}^2(\varphi_{bb}(1 - x_{bb}))^\gamma$, respectively.

We should comment one important difference of the given treatment and previous ones using AW theory to describe the motions of complex polymer systems.[6,7,10,46] In our earlier work, we only distinguished between isotropically mobile segments (defects and chain ends), which were in the final fit accounted for with a separate exponentially decaying contribution to $I_{\Sigma MQ}$ (which will also be added below), and the response of all constrained segments that were considered to behave identically. Here, however, we have to be specifically aware that the NMR signal represents the sum of all protons ("spin counting"), which report on the position-dependent dynamics of their different monomers/segments. Therefore, the total MQ NMR signals ($I_{\Sigma MQ}$, I_{DQ}) are a sum of contributions from each segment, each of which has its own specific correlation function that depends on its position in the hierarchical structure.

The above equations are valid for arm retraction and CLF until $t = \tau_d$ when the reptation process becomes dominant. The normalized OACF in the reptation regime can be expressed as

$$C(t) = S_{b,0}{}^2[\varphi_{bb}(1 - x_d)]^\gamma \sum_{q=odd} \frac{8}{q^2\pi^2}\exp\left[-\frac{q^2 t}{\tau_d(x_d)}\right] \quad (22)$$

The corresponding signal functions read:

$$I_{DQ}^{rept}(\tau_{DQ}, \tau_d(x_d), D_{res,0}) = \exp\left\{\sum_{q=odd} \frac{-8}{q^2\pi^2}0.4[\varphi_{bb}(1 - x_d)]^\gamma D_{res,0}{}^2\left[\frac{\tau_d(x_d)}{q^2}\right]^2 \left[e^{-q^2\tau_{DQ}/\tau_d(x_d)} + \frac{q^2\tau_{DQ}}{\tau_d(x_d)} - 1\right]\right\} \times \sinh\left\{\sum_{q=odd} \frac{8}{q^2\pi^2}0.2[\varphi_{bb}(1 - x_d)]^\gamma D_{res,0}{}^2\left[\frac{\tau_d(x_d)}{q^2}\right]^2 \left[e^{-2q^2\tau_{DQ}/\tau_d(x_d)} - 2e^{-q^2\tau_{DQ}/\tau_d(x_d)} + 1\right]\right\} \quad (23)$$

$$I_{\Sigma MQ}^{rept}(\tau_{DQ}, \tau_d(x_d), D_{res,0}) = \exp\left\{\sum_{q=odd} \frac{-8}{q^2\pi^2}0.2[\varphi_{bb}(1 - x_d)]^\gamma D_{res,0}{}^2\left[\frac{\tau_d(x_d)}{q^2}\right]^2 \left[4e^{-q^2\tau_{DQ}/\tau_d(x_d)} - e^{-2q^2\tau_{DQ}/\tau_d(x_d)} + \frac{2q^2\tau_{DQ}}{\tau_d(x_d)} - 3\right]\right\} \quad (24)$$

The overall signal can be written as the sum of the segmental contributions of arms and backbone:

$$I_{DQ}^{all}(\tau_{DQ}, D_{res}) = \left\{\varphi_a \int_0^1 I_{DQ}^{a}(\tau_{DQ}, \tau(x_a), D_{res}(x_a))dx_a + \varphi_{bb}\left[\int_0^{x_d} I_{DQ}^{bb}(\tau_{DQ}, \tau(x_{bb}), D_{res}(x_{bb}))dx_{bb} + (1 - x_d)I_{DQ}^{rept}(\tau_{DQ}, \tau(x_d), D_{res,0})\right]\right\} \times (1 - \varphi_{tail})e^{-2\tau_{DQ}/T_2} \quad (25)$$

$$I_{\Sigma MQ}^{all} = \left\{\varphi_a \int_0^1 I_{\Sigma MQ}^{a}(\tau_{DQ}, \tau(x_a), D_{res}(x_a))dx_a + \varphi_{bb}\left[\int_0^{x_d} I_{\Sigma MQ}^{bb}(\tau_{DQ}, \tau(x_{bb}), D_{res}(x_{bb}))dx_{bb} + (1 - x_d)I_{\Sigma MQ}^{rept}(\tau_{DQ}, \tau(x_d), D_{res,0})\right]\right\} \times (1 - \varphi_{tail})e^{-2\tau_{DQ}/T_2} + \varphi_{tail}e^{-2\tau_{DQ}/T_{2,tail}} \quad (26)$$

By considering the transverse (T_2) relaxation effect arising from faster intrasegmental motions that are not modeled explicitly and likely identical for arms and backbone, and assuming a slowly relaxing component fraction φ_{tail} representing the isotropic moieties (tail), the DQ signals can be fitted to extract the structural information on a branched polymer (e.g., a comb). In fact, effects leading to distinguishable and separable "tail" responses in NMR experiments, mostly chain-end effects attributed to contour-length fluctuations,[5] have long been known and studied systematically as a function of molecular weight and temperature by e.g., Kimmich[47] and Cohen-Addad.[48] The given approach is novel as for the first time, complex position-dependent segmental dynamics with a solid foundation in rheology theory is incorporated into NMR theory.

We finally note on a subject creating ongoing confusion in the perception of NMR results by the polymer community. The long-time decay of the above NMR signal functions, with the explicitly calculated polymer-specific nonexponential contributions as well as the ad-hoc exponential T_2 terms, is commonly referred to as *transverse relaxation*. The dependence of this phenomenon (and also of longitudinal spin−spin relaxation, T_1) on actual molecular dynamics time scales is obviously highly nonlinear, often even nonmonotonic. It *must not be confused* with the use of the term "relaxation" in the context of polymer dynamics in the time domain, where it is a direct, mostly (multi)exponential reflection of the correlation time of motion.

EXPERIMENTAL SECTION

Material. A monodisperse polyisoprene comb polymer was synthesized via anionic polymerization and characterized by size-

https://doi.org/10.1021/acs.macromol.4c02015
Macromolecules 2024, 57, 11030−11041

exclusion chromatography with combined multiangle laser light scattering (SEC-MALLS), with details given in the Supporting Information (SI), SI1 and Figure S1. In the comb polymer structure, the backbone and the arm length M_b and M_a are 68 and 13.8 kg/mol, respectively, both with a polydispersity (PD) of 1.1. The overall molecular weight of the comb is M_c = 189 kg/mol with PD = 1.06. On average, each backbone thus carries 8.5 arms, so the overall fraction of arm segments φ_a is 63%.[49]

Rheology. Small-amplitude oscillatory shear measurements were carried out using ARES-G2 rheometer with a 13 mm parallel plate geometry from 100 to 1 rad/s at temperature range between −40 to 110 °C. A master curve was constructed via time−temperature superposition for T_{ref} = 0 °C, above the T_g of −59 °C. The fit of the horizontal shift factors to the Williams−Landel−Ferry (WLF) equation provided the WLF constants C_1 = 6.30 and C_2 = 118 K.

NMR. The PI-comb samples were measured in a sealed 5 mm NMR glass tube on a 400 MHz (9.4 T) Bruker Avance III spectrometer with 90° pulse and 180° pulses of 4 and 8 μs, respectively, using a static probe. A BVT3000 temperature control unit regulated the sample temperature via an airflow with an accuracy of 0.5 K.

RESULTS AND DISCUSSION

The explained DTD model is being applied to evaluate the rheological and MQ NMR data. The main aim is to identify the correct correlation between the segmental order parameter and entanglement length. By fixing the chain structure parameters (like the number of arms and the molecular weight of the arm and backbone), the obtained tube model-related constants, i.e., τ_e, the entanglement time, and M_e, the entanglement molecular weight, will be compared to the reported values by previous studies to assess the interpretation of the DTD as applied to NMR-based OACF.

The rheological measurement of the comb PI sample is shown in Figure 2. At very high angular frequency, the Rouse relaxation can be seen, continuing into the entanglement rubbery plateau. In this regime, a hypothetical tube that represents the restriction applied by the neighboring chains is assumed. Since the arm's tube is on average perpendicular to the backbone, the reptation motion in the backbone can be executed only after the relaxation of the arms. In the first plateau, the dynamic behavior is governed by the retraction motion of the arms and contour length fluctuation in the outer backbone segments. This regime lasts until the arms relax entirely and the backbone can start its reptation motion. This can be seen at the very low angular frequency when the chains enter the free-diffusion regime.

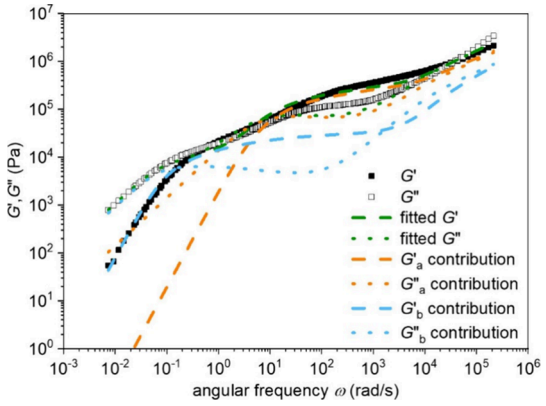

Figure 2. Rheological master curve constructed via TTS at T_{ref} = 0 °C. Green lines correspond to the best-fit line based on the suggested interpretation of DTD assumption for monodisperse comb polymer. Contribution of the arm and backbone segments are depicted separately.

The DTD model according to eqs 4−7 was applied to fit the rheological responses in Figure 2, using the known molecular weight and topological parameters. The best-fit values of G_N, τ_e, and M_e are listed in Table 1. As seen, all the obtained parameters are in the range previously reported by other researchers.

Figure 2 also shows the best-fit model and the contributions of the backbone and arm in storage modulus. As observed, the best-fit storage and loss moduli fit the data with reasonable precision. By comparing the arms and backbone's contribution, it can be understood that the arm contribution fits the first plateau, whereas, after the relaxation of the arms, the storage modulus is governed by the backbone relaxation. At the high frequencies, a significant difference between the contributions of arms and backbone is observed.

According to the rubber elasticity and tube models, the plateau modulus is proportional to the number of entanglement strands per unit volume. As already discussed, the number of entanglements is assumed as a function of unrelaxed segment fraction in the DTD assumption. Therefore, the average mechanical load taken by entangled segments of unrelaxed arms and the backbone should be identical. The contribution of the backbone and arms in the moduli depends on the fraction of each. To remove this dependency, the storage modulus per segment is defined, i.e., the storage modulus contribution of the arms or backbone divided by the associated fraction, $G^{seg}_{a,b} = G_{a,b}/f_{a,b}$. Since the mechanical behavior in the Rouse regime arises from the segmental motion shorter than the entanglement length, the storage modulus per segment should be identical for the backbone and arms, while in the limit of low frequencies, it should approach zero for arms. For a better understanding, Figure 3 shows the ratio of the storage modulus per segment in the arms to the storage modulus per segment in a backbone.

As it is seen in Figure 3, all the arm segments have indeed relaxed at low frequencies, and the ratio equals zero on the left-hand side of the plot. In the Rouse regime, this ratio is close to 1 at very high frequencies. At midrange frequency, this ratio increases and passes a maximum. Considering that the backbone segments relax slower than the arms, the mentioned trend is physically not entirely reasonable. It is expected that the contribution of arm segments becomes weaker due to faster relaxation. This may indicate a shortcoming of the suggested interpretation of the DTD assumption for monodisperse comb polymers.[32] Thus, it can be concluded that the DTD model modified for comb polymers, constructed under the assumption of fast but not correlated averaging, may not have physical meaning for the separated contributions.

Table 1. Best-Fit Tube Parameters of the Rheological Master Cuves (T_{ref} = 0 °C) and Reference Values From Previous Works

fitting parameter	best-fit value	value from previous work[30,32]
G_0 (MPa)	0.39	0.36−0.44
τ_e (s)[a]	1.5×10^{-5}	$0.7-1.5 \times 10^{-5}$
M_e (g/mol)[b]	4329	4000−5000

[a]Shifted to 25 °C to be comparable with values from previous works. [b]M_e is not a fitting parameter but is determined by G_0

https://doi.org/10.1021/acs.macromol.4c02015
Macromolecules 2024, 57, 11030−11041

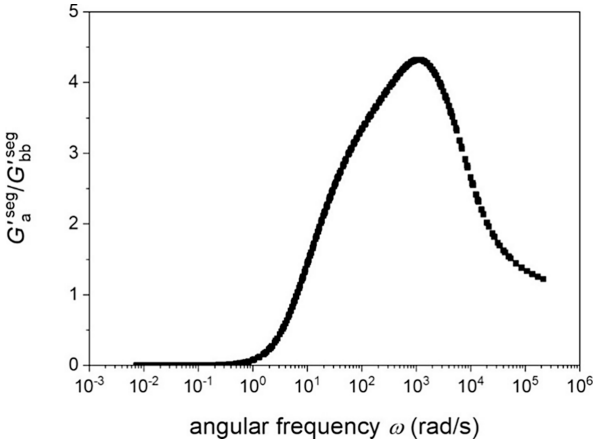

Figure 3. Ratio of storage modulus per segment in arms vs backbone (contribution of arm segment in storage modulus per contribution of backbone segment in storage modulus) obtained from the DTD model best-fit parameters (Table 1) versus angular frequency (T_{ref} = 0 °C).

The mentioned averaging follows from the suggested interpretation of the DTD model[32] in a monodisperse comb polymer. It is correctly assumed that when the backbone's segments start the relaxation process, the whole arms have already relaxed. However, the model uses the same unrelaxed-segments fraction for times shorter than the relaxation of the arms. In other words, a diluted modulus is used for backbone segments at high frequencies, which might be questionable. This problem results in an underestimation of the contribution of the backbone segments in storage and loss moduli. In the following, the interpretation of this method in fitting MQ NMR data will be assessed, keeping in mind this apparent shortcoming.

MQ NMR Measurements of Comb PI. The MQ NMR data is fitted with the NMR-modified DTD model. As seen in eqs 18 and 19, an exponential correlation function is assumed for each segment with a unique relaxation time determined based on the segmental curvilinear dimensionless coordinate. It is assumed that the order parameter correlates with the inverse of entanglement length with the power of 1 or 1/2 (see theoretical background), but in this section, we only assume the exponent 1 for checking the OACF (free fitting of the exponent proved ambiguous).

In the DTD model modified for polymer comb, the unrelaxed-segments fraction of arms and backbone are $(1 - \varphi_a x_a)$ and $\varphi_b(1 - x_b)$, respectively. In other words, the unrelaxed segment fraction is written as a function of the segmental curvilinear dimensionless coordinate. Unlike for rheology, where the relaxed segments do not have any observable response, in MQ NMR, the relaxed segments show a slowly decaying signal tail at long times. Since the Anderson-Weiss approximation is not accurate for isotropic moieties, a tail fraction should be defined for the relaxed segments. Accordingly, the segments with relaxation times shorter than the first recorded τ_{DQ} are considered defects with a long transverse relaxation time that can be accounted for by a separate component of the fitting function.

Table 2 lists the best-fit parameters obtained via fitting the MQ NMR data with the positional-dependent unrelaxed-segments fraction. It is seen that the entanglement length is close to the reference range; however, the entanglement equilibration time is approximately 1 order of magnitude slower than the reported values.

Table 2. Best-Fit Parameters Resulting From the Simultaneous Fitting of the MQ NMR Data at Eight Different Temperatures Using TTS (T_{ref} = 0°C)

fitting parameter	best-fit value	value from previous work[30,32]
τ_e (s)[a]	2×10^{-4}	$0.7-1.5 \times 10^{-5}$
M_e (g/mol)	3995	4000−5000

[a]Shifted to 25 °C to be comparable with values from previous works.

Figure 4 shows the simultaneous fitting of ΣMQ and DQ signals measured at two different temperatures (30 °C, 60 °C) using TTS at 0 °C as the reference temperature. Since the Andersson-Weiss approximation becomes increasingly inaccurate for experimental times much beyond the DQ intensity maximum, the DQ signals are fitted until the blue vertical line marking the τ_{DQ} at the maximum DQ signal. The fraction of relaxed segments increases with increasing temperature due to the enhanced segmental dynamics. As it is observed, at 30 °C, the best-fit line can fit the data in the fitting interval rather well, whereas at 60 °C, the fits more significantly, particularly in DQ signals around its maximum deviate and in ΣMQ signals at long times (tail signal).

Figure 5 demonstrates the constructed segmental OACF based on the best-fit parameters, shown in Table 2. As it is highlighted on the time axis, more than five decades are covered by the MQ NMR technique using TTS. The highest OACF value belongs to the outermost segment of the arm, and the lowest one is associated with the segments relaxing via reptation motion in the backbone. At very short times in the left-hand side of Figure 5, 2 orders of magnitude difference between the OACF associated with the outermost arm segment and innermost backbone segment is observed. Since the OACF is assumed to be proportional to the inverse of the squared entanglement length, it means that the entanglement length in the innermost backbone part is even initially ten times larger than in the outermost arm segments, which cannot be correct. In other words, the time scale of the dynamic dilution effect on a given segment is neglected. The plotted OACF clearly illustrate the lack of physical meaning of the suggested interpretation of the DTD assumption for monodisperse comb polymers.[30,32]

In rheology, the model focused on fitting the first plateau by arm relaxation and the second one with backbone relaxation without any concern about the contribution of the backbone segments in the first plateau region. This leads to an underestimation of the backbone contribution that is in the end not relevant in obtaining reasonable fitting results. While thus not posing a relevant problem for fitting the rheology data of a monodisperse comb, it leads to a significant systematic error for parameters derived from MQ NMR signals. Unlike in rheology, the magnitude of the OACF affects the NMR signal relaxation times and leads to a significantly shifted best-fit entanglement time, as seen in Table 2.

Since this incorrect picture is the result of using time-independent unrelaxed-segments fraction ($\varphi_b(1 - x_b)$ in the backbone), we now assume a time-dependent unrelaxed-segments fraction to fit the rheological and MQ NMR data in the following.

Time-Dependent Unrelaxed-Segments Fraction: Rheology. In order to render the modeling of the correlation function more accurate, the unrelaxed-segments fraction can be

https://doi.org/10.1021/acs.macromol.4c02015
Macromolecules 2024, 57, 11030−11041

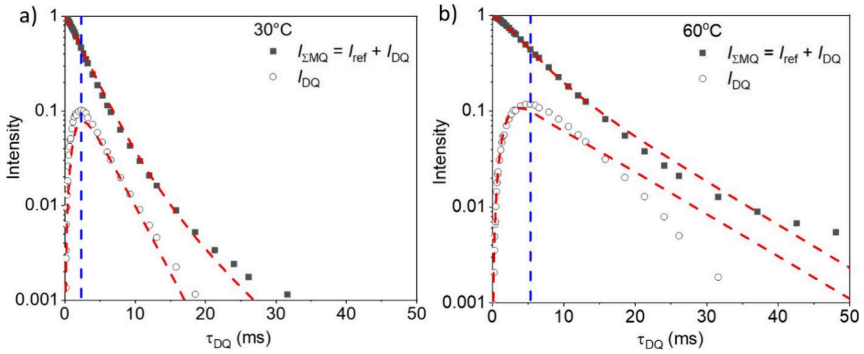

Figure 4. Simultaneous fitting of the MQ NMR data measured at (a) 30 °C and (b) 60 °C. It is noted that the data were measured at eight different temperatures, from 30 to 90 °C with 10 °C intervals. Red and blue dashed lines show the best-fit model and the fitting interval of the DQ signal, respectively. Thus, the fit represents a prediction for times beyond the blue dashed line.

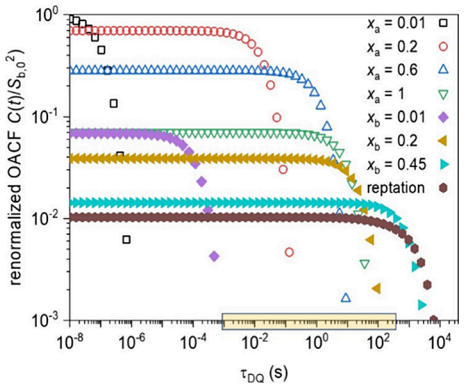

Figure 5. Segmental OACF for different positions along the chains using eqs 18, 19, 22 obtained at T_{ref} = 0 °C from the best-fit parameters in Table 2. Highlighted part of the time axis shows the covered time range by MQ NMR data using TTS. In fitting the data, 100 segmental parts have been assumed in the arms and backbone.

considered as an explicit function of time. A time-dependent unrelaxed-segments fraction has in fact been used in the improved, so-called hierarchical relaxation model to study polydisperse branched polymer and the blend of linear and star polymers.[21−24] In the mentioned model, the potential of the arm retraction and backbone contour length fluctuation depends on the time-dependent unrelaxed segment fraction, obviously a more physical choice. In our case, as a monodisperse comb-polymer, it is not necessary to alter the relaxation time hierarchy because the segmental-position-dependent unrelaxed-segments fraction is valid for use in the potential function. We only need to define the time-dependent unrelaxed-segments fraction for use in moduli or correlation functions to check consistency with the rheological response and then use it for MQ NMR data. The general expression for the time-dependent modulus is

$$G(t) = \int_{\tau_i}^{\tau_f} \frac{\partial G_N(\tau)}{\partial \tau} \exp\left(-\frac{t}{\tau}\right) d\tau \tag{27}$$

Since the diluted modulus is defined as $G_N(\tau) = G_N^0[\Phi(\tau)]^{\alpha+1}$, eq 27 turns into:

$$G(t) = G_N^0(1+\alpha)\int_{\tau_i}^{\tau_f} [\Phi(\tau)]^{\alpha} \exp\left(-\frac{t}{\tau}\right)\frac{\partial \Phi(\tau)}{\partial \tau} d\tau = G_N^0(1+\alpha)\int_0^1 [\Phi(\tau)]^{\alpha} \exp\left(-\frac{t}{\tau}\right) d\Phi \tag{28}$$

The Fourier transform of the exponential decays in this expression provides Lorentzians (as in the simple Maxwell model), so the frequency-dependent dynamical responses can be written as

$$\frac{G'(\omega)}{G_N^0} = (1+\alpha)\int_0^1 \frac{\omega^2\tau^2}{1+\omega^2\tau^2}[\Phi(\tau)]^{\alpha} d\Phi \tag{29}$$

$$\frac{G''(\omega)}{G_N^0} = (1+\alpha)\int_0^1 \frac{\omega\tau}{1+\omega^2\tau^2}[\Phi(\tau)]^{\alpha} d\Phi \tag{30}$$

The best-fit parameter obtained via time-dependent unrelaxed-segments fraction can be found in Table 3. The model predicts the G_0, τ_e, and M_e in the same range reported by the previous works, illustrating the minor role of the unrelaxed-segments fraction.

Figure 6 shows the rheological data and best-fit model according to eqs 29 and 30. The best-fit line predicts the dynamic behavior of the polymer comb in the whole studied frequency range satisfactorily. A deviation from experimental data of up to a factor 2 is observed in the midrange frequency in which the outermost part of the backbone and the innermost part of the arm relax simultaneously. A similarly large deviation has also been observed in the same frequency range in Figure 2, but to a somewhat lesser degree for G'.

At very high frequencies, the arm contribution in moduli is higher than the backbone's, which is understandable according to the higher fraction of arm segments (ca. 63%). Due to the relaxation of arm segments, the arm contribution decreases and gradually disappears at very low frequencies. In this frequency

Table 3. Best-Fit Tube Parameters of the Rheological Master Curves (T_{ref} = 0 °C) Assuming a Time-Dependent Unrelaxed-Segments Fraction

fitting parameter	best-fit value	value from previous work[30,32]
G_0 (MPa)	0.35	0.36−0.44
τ_e (s)[a]	1.8×10^{-5}	$0.7-1.5 \times 10^{-5}$
M_e (g/mol)	4814	4000−5000

[a]Shifted to 25 °C to be comparable with values from previous works.

https://doi.org/10.1021/acs.macromol.4c02015
Macromolecules 2024, 57, 11030−11041

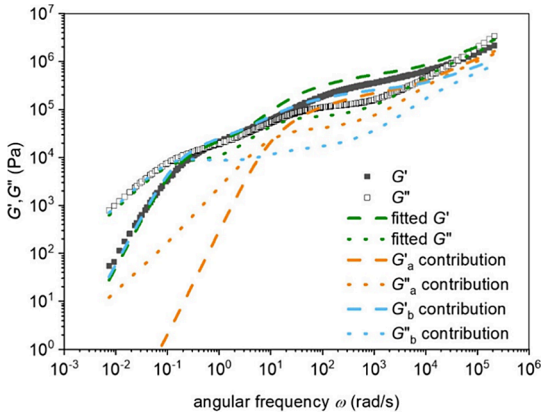

Figure 6. Rheological master curve constructed via TTS at T_{ref} = 0 °C. Green lines correspond to the best fit resulting from the DTD model with time-dependent unrelaxed-segments fraction. Contribution of the arm and backbone segments are depicted separately.

range, the dynamic behavior is mainly governed by the backbone segments. As compared to the decomposition shown in Figure 2, the current relative magnitude of the contributions of arm and backbone chains appear physically more plausible.

To illustrate this more clearly, Figure 7a shows the ratio of the storage modulus per segment in arms to the storage modulus per segment in the backbone against angular frequency. At very high frequencies, when only a minority of arm segments has already relaxed, this ratio is highest. The arm relaxation rate increases at lower frequencies, and a decay is observed, leading to a plateau in the midrange frequencies (5000 to 100 rad/s). This plateau results from increasing the number of backbone segments relaxing via CLF in the mentioned frequency range. This can be seen clearly in Figure 7b. At low frequencies, the reptation motion in the backbone becomes dominant, and the whole system enters the free-diffusion regime. This cannot be seen in Figure 7a because the arm contribution disappears at 1 rad/s.

Time-Dependent Unrelaxed-Segments Fraction: MQ NMR. As discussed so far, for fitting the MQ NMR data according to the DTD assumption, it is necessary to use time-dependent unrelaxed-segments fraction. This time-dependent fraction can be written as

$$\Phi(t) = \varphi_a\left[\int_0^1 \exp(-\frac{t}{\tau_a(x_a)})dx_a\right] + \varphi_{bb}\left\{\int_0^{x_d} \exp\left[-\frac{t}{\tau_{bb}(x_{bb})}\right]dx_{bb} + (1 - x_d)\right\} \quad (31)$$

It is divided into the arm and backbone segments. In arms, the only relaxation process is arm retraction, whereas, in the backbone, the outer part of the chain relaxes via the CLF process, and the inner part (from x_d to 1) follows reptation motion.

Since the chains are considered a finite set of segments, the integral can be transformed into a summation:

$$\Phi(t) = \varphi_a\left\{\frac{1}{n}\sum_{i=1}^{n} \exp\left[-\frac{t}{\tau_a(i/n)}\right]\right\} + \varphi_{bb}\left\{\frac{1}{n}\sum_{i=1}^{n_d} \exp\left[-\frac{t}{\tau_{bb}(i/n)}\right] + (1 - x_d)\right\} \quad (32)$$

The reptation motion is the final relaxation process, which means the innermost of the backbone $(1 - x_d)$, relaxes after the relaxation of all other segments. By replacing the unrelaxed-segments fraction in eq 17, the OACF becomes

$$C(t, x_{a,b}) = S_{b,0}{}^2\left\{\varphi_a\frac{1}{n}\sum_{i=1}^{n} \exp\left[-\frac{t}{\tau_a(i/n)}\right] + \varphi_{bb}\frac{1}{n}\sum_{i=1}^{n_d} \exp\left[-\frac{t}{\tau_{bb}(i/n)}\right] + (1 - x_d)\right\}^{\gamma} \exp\left[-\frac{t}{\tau_{a,bb}(x_{a,bb})}\right] \quad (33)$$

The above equation represents the OACF based on the DTD assumption with a time-dependent unrelaxed-segments fraction. As discussed, γ can be equal to α or 2α, depending on the relation between the order parameter and the entanglement length.

It was explained that for determining the signal functions, the phases during DQ NMR time evolution are determined by an integral over this time (resulting from the AW approximation). To have explicit signal functions, we have to rewrite the OACF in the form of a summation of single exponential functions (to be able to solve the integrals

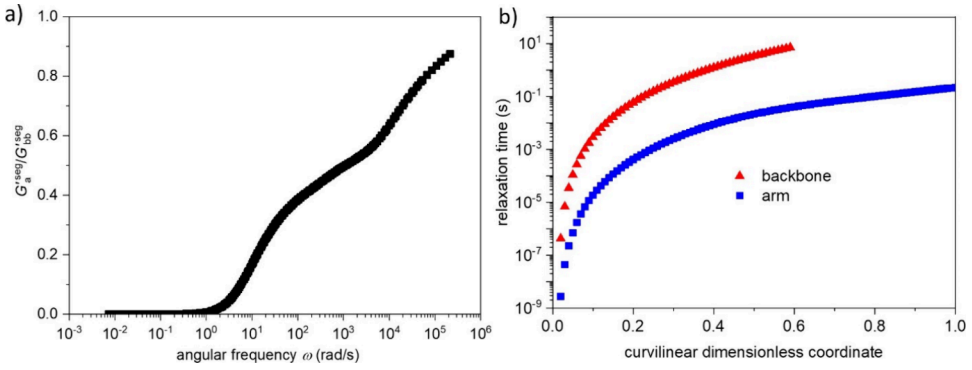

Figure 7. (a) Ratio of storage modulus per segment in arms vs backbone (contribution of arm segment in storage modulus per contribution of backbone segment in storage modulus) obtained from the best-fit model shown in Table 3 versus angular frequency. (b) Hierarchy of the relaxation times according to the curvilinear dimensionless coordinate.

https://doi.org/10.1021/acs.macromol.4c02015
Macromolecules 2024, 57, 11030−11041

analytically); otherwise, we have to fit the data by determining the signal functions via lengthy numerical integration.

It is clear that for noninteger values of γ, the integrals cannot be solved analytically. Moreover, for $\gamma = 2$, the number of terms increases significantly, and the numerical approach would probably be a better option (in the case of expanding the summation as it was done for $\gamma = 1$). Nevertheless, for $\gamma = 1$, the signal functions can be calculated analytically which is shown in detail in the Supporting Information S2.

In Table 4, the best-fit model parameters are listed for different α, $\gamma = \alpha$ or 2α, and different p^2 values. See the Theory section under "Relaxation spectrum of comb polymers" for an explanation of this parameter. In previous works, p^2 has been taken as either 1/12 or 1/40.[24,30] While the former value was assumed in our analyses so far, we here consider also the latter value, demonstrating its minor influence. For γ values other than 1, the fittings were done via time-consuming numerical integration. Unlike rheology, the entanglement length is a fitting parameter in the MQ NMR data because for writing an explicit relation between D_{res} and entanglement length according to equation 8, the k and D_{stat} values need to be determined on the basis of molecular models using simplified assumptions. In this light, the determined values are model-dependent and may systematically deviate from rheology results.

For all fittings, obtained D_{res} values are in a narrow range, while the other fitting parameters vary more strongly. Comparing the best-fit parameters with the reference data obtained in previous studies shows that the fittings with $\gamma = 1$ provide consistent results. Notably, the theoretical NMR-based $\gamma = 2$ (or 8/3) failed to predict the PI-comb's dynamics. The latter exponent value has been obtained based on the relation between the order parameter and entanglement length (in polymer melts) or cross-link density (in polymer networks), while $\gamma = 1$ has been taken from the analogy between the current system and a lowly cross-linked polymer network studied by Lang and Sommer.[1] They reported that according to the molecular simulation, the order parameter of an entangled chain between two cross-links correlates with the inverse square root of entanglement length and the number of segments between two cross-links ($S_b \sim 1/\sqrt{NN_e}$), which deviates from the classical relation of the order parameter, $S_b \sim \frac{1}{N} + \frac{1}{N_e}$. Our results showed that the linear relation between the order parameter and the inverse of the entanglement length is indeed not fully correct. It is noted that the analogy used here is valid for backbone segments over a wide time range, while it may not be entirely correct for the arms relaxing from a free end.

The fits of the improved DTD model to the NMR data, provided in the SI3 (Figure S2), show a general resemblance to those obtained from the rather unphysical simple version. However, the deviations of this still-simplistic model from the NMR data are not significantly greater than the deviations observed when comparing the model to rheology data.

Figure 8 shows the normalized OACF constructed using TTS by fitting MQ NMR data with time-dependent unrelaxed-segments fraction over almost 12 decades. Unlike the previous fitting approach (time-independent unrelaxed-segments fraction), it is seen that all the segments start at a common normalized amplitude until the onset of relaxation process via arm retraction, CLF, or reptation. The relaxation starts from the outermost segments of the arms. As the innermost arm segment relaxes, the second plateau appears, which is governed by the inner parts of the backbone. At the longest times, the whole chain relaxes via reptation.

Table 4. Tube Model Parameters Obtained From MQ NMR Data with the DTD Model Including a Time-Dependent Unrelaxed-Segments Fraction (T_{ref} = 0 °C)

parameters	D_{res} (Hz)	τ_e (s)[a]	M_e (g/mol)
$\alpha = 1$ $p^2 = 1/40$ $\gamma = 1$	287	1×10^{-5}	4154
$\alpha = 1$ $p^2 = 1/12$ $\gamma = 1$	251	1.8×10^{-5}	3822
$\alpha = 4/3$ $p^2 = 1/12$ $\gamma = 8/3$	279	1.9×10^{-6}	1754
$\alpha = 1$ $p^2 = 1/40$ $\gamma = 2$	291	1.6×10^{-6}	2115
ref. values[30,32]		$0.7-1.5 \times 10^{-5}$	4000−5000

[a]Shifted to 25 °C to be comparable with values from previous works.

CONCLUSIONS

In order to investigate the correlation between the segmental order parameter and entanglement length in lowly cross-linked networks, the chain dynamics of a monodisperse polyisoprene comb (as an analogous system) were studied via rheology and melt-state ^{1}H MQ NMR. The data was analyzed using the DTD model, which has been used to characterize the chain dynamics in star and branched polymers from rheology data. The core of this theory is that the dilution effect arises from the relaxed chains, increasing the entanglement length and the tube diameter. The DTD model predicted the rheological behavior of the sample qualitatively correctly, but it is observed that the contribution of the backbone segments in storage

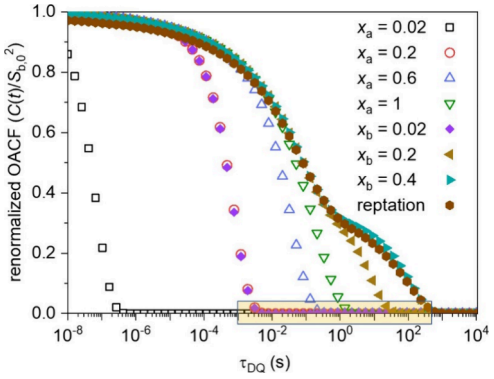

Figure 8. Segmental OACF for different positions along the chains using eqs 18, 19, 22 from the best-fit model parameters in Table 4 ($\alpha = 1$, $p^2 = 1/40$, $\gamma = 1$), obtained at T_{ref} = 0 °C. The highlighted time axis shows the covered time range by MQ NMR data using TTS. In fitting the data, 50 segmental parts have been assumed in the summations for arms and backbone.

https://doi.org/10.1021/acs.macromol.4c02015
Macromolecules 2024, 57, 11030−11041

modulus is significantly underestimated at high frequencies. In MQ NMR data, this leads to a completely unrealistic picture for the OACF, where the time scale of the dynamic dilution effect of the fast-relaxing components (outer parts of the arms) on the relaxation of the inner parts is simply ignored.

This problem arises from the assumption that considers the unrelaxed-segments fraction as a sole function of the segmental dimensionless coordinate (time-independent function). This was modified by considering a time-dependent unrelaxed-segments fraction in the DTD model. Via this modification, the DTD model predicted the rheological behavior with a physically reasonable contribution of arm and backbone in storage modulus in the studied frequency range.

To assess the relation between the segmental order parameter S_b as the MQ NMR observable and the (diluted) entanglement length N_e, two possible scaling exponents $S_b \sim N_e^{-1}$ and $\sim N_e^{-0.5}$ were considered for the improved fit to the MQ NMR data. The results demonstrated that the former classical relation between the order parameter and entanglement length is not valid in the studied case. Instead, our results confirm the findings of Lang and Sommer,[1] who reported that the order parameter correlates with the square-root of inverse entanglement length in a lowly cross-linked polymer system.

The results showed that the MQ NMR technique can be used for probing the branched (thus also star) polymers via the DTD model. MQ NMR probes the chain dynamics on a time scale being one decade and a half faster than rheology. Moreover, the segments with very fast relaxation times (faster than the studied time window) can be probed in the MQ signal (as a tail signal). Since in polyolefins, the segmental dynamics are fast, and the rheological measurement is restricted by the crystallization of the chains at low temperatures, the MQ NMR experiment can be a complementary technique to assess these polymeric systems. The current research represents the first attempt to apply the DTD model in the MQ NMR technique.

Beyond the importance of this work within the tube model framework, the methodology developed in this research for evaluating MQ NMR signals to probe the dynamics of each segment solely with a unique relaxation time has been done for the first time. This method can provide new insights into studying chain dynamics in systems with position-dependent relaxation time profile. Specifically, it can be practically applied to extract the relaxation time profile of confined polymer chains in polymer (nano)composites using MQ NMR technique as a "molecular rheology" tool.

■ ASSOCIATED CONTENT

Data Availability Statement

The data sets generated and analyzed for this study as they appear in the figures of this article and the Supporting Information can be found in the Zenodo repository, DOI: 10.5281/zenodo.13342840. The Python codes used for data fitting have been published in the dissertation of F.S., DOI: 10.25673/112369. Further details on the sample preparation and characterization, including also dielectric spectroscopy results, are found in the dissertation of J.K., DOI: 10.5445/IR/1000132803.

Supporting Information

The Supporting Information is available free of charge at https://pubs.acs.org/doi/10.1021/acs.macromol.4c02015.

Synthesis and characterization details, derivation of MQ NMR signal functions with time-dependent unrelaxed-segments fraction, and fitting of MQ NMR data with the improved DTD model (PDF)

■ AUTHOR INFORMATION

Corresponding Authors

Farhad Shahsavan − *Institut für Physik−NMR, Martin-Luther-Universität Halle-Wittenberg, 06120 Halle (Saale), Germany*; Email: farhad.shahsavan@gmail.com

Kay Saalwächter − *Institut für Physik−NMR, Martin-Luther-Universität Halle-Wittenberg, 06120 Halle (Saale), Germany*; orcid.org/0000-0002-6246-4770; Email: kay.saalwaechter@physik.uni-halle.de

Authors

Jonas Keller − *Institute for Chemical Technology and Polymer Chemistry, Karlsruhe Institute of Technology (KIT), 76131 Karlsruhe, Germany*

Manfred Wilhelm − *Institute for Chemical Technology and Polymer Chemistry, Karlsruhe Institute of Technology (KIT), 76131 Karlsruhe, Germany*; orcid.org/0000-0003-2105-6946

Complete contact information is available at: https://pubs.acs.org/10.1021/acs.macromol.4c02015

Notes

The authors declare no competing financial interest.

■ ACKNOWLEDGMENTS

Financial support by the Deutsche Forschungsgemeinschaft (DFG) through grants SA 982/11-1 and WI 1911/23-1 is gratefully acknowledged.

■ DEDICATION

This article is dedicated to Nail Fatkullin on the occasion of his 70th birthday.

■ REFERENCES

(1) Lang, M.; Sommer, J.-U. Analysis of entanglement length and segmental order parameter in polymer networks. *Phys. Rev. Lett.* **2010**, *104* (17), No. 177801.

(2) de Gennes, P.-G. Reptation of a polymer chain in the presence of fixed obstacles. *J. Chem. Phys.* **1971**, *55* (2), 572−579.

(3) Doi, M.; Edwards, S. F. *The theory of polymer dynamics*; Oxford University Press, 1988.

(4) Saalwächter, K. Proton multiple-quantum NMR for the study of chain dynamics and structural constraints in polymeric soft materials. *Prog. Nucl. Magn. Reson. Spectrosc.* **2007**, *51* (1), 1−35.

(5) Vaca Chávez, F.; Saalwächter, K. Time-Domain NMR Observation of Entangled Polymer Dynamics: Universal Behavior of Flexible Homopolymers and Applicability of the Tube Model. *Macromolecules* **2011**, *44* (6), 1549−1559.

(6) Vaca Chávez, F.; Saalwächter, K. Time-Domain NMR Observation of Entangled Polymer Dynamics: Analytical Theory of Signal Functions. *Macromolecules* **2011**, *44* (6), 1560−1569.

(7) Saalwächter, K.; Heuer, A. Chain Dynamics in Elastomers As Investigated by Proton Multiple-Quantum NMR. *Macromolecules* **2006**, *39* (9), 3291−3303.

(8) Vaca Chávez, F.; Saalwächter, K. NMR observation of entangled polymer dynamics: tube model predictions and constraint release. *Phys. Rev. Lett.* **2010**, *104* (19), No. 198305.

(9) Trutschel, M.-L.; Mordvinkin, A.; Furtado, F.; Willner, L.; Saalwächter, K. Time-domain NMR observation of entangled polymer dynamics: Focus on all tube-model regimes, chain center, and matrix effects. *Macromolecules* **2018**, *51* (11), 4108−4117.

(10) Mordvinkin, A.; Suckow, M.; Böhme, F.; Colby, R. H.; Creton, C.; Saalwächter, K. Hierarchical sticker and sticky chain dynamics in self-healing butyl rubber ionomers. *Macromolecules* **2019**, *52* (11), 4169−4184.
(11) Mordvinkin, A.; Döhler, D.; Binder, W. H.; Colby, R. H.; Saalwächter, K. Terminal Flow of Cluster-Forming Supramolecular Polymer Networks: Single-Chain Relaxation or Micelle Reorganization? *Phys. Rev. Lett.* **2020**, *125* (12), No. 127801.
(12) Shahsavan, F.; Beiner, M.; Saalwächter, K. Chain dynamics in partially cross-linked polyethylene by combined rheology and NMR-based molecular rheology. *J. Polym. Sci.* **2022**, *60* (7), 1266−1276.
(13) Saalwächter, K.; Herrero, B.; López-Manchado, M. A. Chain order and cross-link density of elastomers as investigated by proton multiple-quantum NMR. *Macromolecules* **2005**, *38* (23), 9650−9660.
(14) Chassé, W.; López Valentín, J.; Genesky, G. D.; Cohen, C.; Saalwächter, K. Precise dipolar coupling constant distribution analysis in proton multiple-quantum NMR of elastomers. *J. Chem. Phys.* **2011**, *134* (4), 44907.
(15) Chasse, W.; Lang, M.; Sommer, J.-U.; Saalwachter, K. Cross-link density estimation of PDMS networks with precise consideration of networks defects. *Macromolecules* **2012**, *45* (2), 899−912.
(16) Valentín, J. L.; Carretero-González, J.; Mora-Barrantes, I.; Chassé, W.; Saalwächter, K. Uncertainties in the determination of cross-link density by equilibrium swelling experiments in natural rubber. *Macromolecules* **2008**, *41* (13), 4717−4729.
(17) Karekar, A.; Oßwald, K.; Reincke, K.; Langer, B.; Saalwächter, K. NMR studies on the phase-resolved evolution of cross-link densities in thermo-oxidatively aged elastomer blends. *Macromolecules* **2020**, *53* (24), 11166−11177.
(18) Lange, F.; Schwenke, K.; Kurakazu, M.; Akagi, Y.; Chung, U.; Lang, M.; Sommer, J.-U.; Sakai, T.; Saalwächter, K. Connectivity and Structural Defects in Model Hydrogels: A Combined Proton NMR and Monte Carlo Simulation Study. *Macromolecules* **2011**, *44* (24), 9666−9674.
(19) Sotta, P.; Fülber, C.; Demco, De; Blümich, B.; Spiess, H. W. Effect of residual dipolar interactions on the NMR relaxation in cross-linked elastomers. *Macromolecules* **1996**, *29* (19), 6222−6230.
(20) Chassé, W.; Schlögl, S.; Riess, G.; Saalwächter, K. Inhomogeneities and local chain stretching in partially swollen networks. *Soft Matter* **2013**, *9* (29), 6943−6954.
(21) Wang, Z.; Chen, X.; Larson, R. G. Comparing tube models for predicting the linear rheology of branched polymer melts. *J. Rheol.* **2010**, *54* (2), 223−260.
(22) Park, S. J.; Shanbhag, S.; Larson, R. G. A hierarchical algorithm for predicting the linear viscoelastic properties of polymer melts with long-chain branching. *Rheologica Acta* **2005**, *44* (3), 319−330.
(23) Larson, R. G. Combinatorial rheology of branched polymer melts. *Macromolecules* **2001**, *34* (13), 4556−4571.
(24) Das, C.; Inkson, N. J.; Read, D. J.; Kelmanson, M. A.; McLeish, T. C. B. Computational linear rheology of general branch-on-branch polymers. *J. Rheol.* **2006**, *50* (2), 207−234.
(25) Daniels; McLeish, T. C.; Crosby, B. J.; Young, R. N.; Fernyhough, C. M. Molecular rheology of comb polymer melts. 1. Linear viscoelastic response. *Macromolecules* **2001**, *34* (20), 7025−7033.
(26) Pearson, D. S.; Helfand, E. Viscoelastic properties of star-shaped polymers. *Macromolecules* **1984**, *17* (4), 888−895.
(27) Milner, S. T.; McLeish, T. C. Parameter-free theory for stress relaxation in star polymer melts. *Macromolecules* **1997**, *30* (7), 2159−2166.
(28) Ball, R. C.; McLeish, T. C. Dynamic dilution and the viscosity of star-polymer melts. *Macromolecules* **1989**, *22* (4), 1911−1913.
(29) Watanabe, H. Dynamic Tube Dilation in Branched Polymers. *Prog. Theor. Phys. Suppl.* **2008**, *175*, 17−26.
(30) Inkson, N. J.; Graham, R. S.; McLeish, T. C.; Groves, D. J.; Fernyhough, C. M. Viscoelasticity of monodisperse comb polymer melts. *Macromolecules* **2006**, *39* (12), 4217−4227.
(31) Lee, J. H.; Fetters, L. J.; Archer, L. A. Stress relaxation of branched polymers. *Macromolecules* **2005**, *38* (26), 10763−10771.
(32) McLeish, T. C.; Allgaier, J.; Bick, D. K.; Bishko, G.; Biswas, P.; Blackwell, R.; Blottiere, B.; Clarke, N.; Gibbs, B.; Groves, D. J. Dynamics of entangled H-polymers: Theory, rheology, and neutron-scattering. *Macromolecules* **1999**, *32* (20), 6734−6758.
(33) Daniels, D. R.; McLeish, T. C. B.; Kant, R.; Crosby, B. J.; Young, R. N.; Pryke, A.; Allgaier, J.; Groves, D. J.; Hawkins, R. J. Linear rheology of diluted linear, star and model long chain branched polymer melts. *Rheologica Acta* **2001**, *40* (5), 403−415.
(34) van Ruymbeke, E.; Masubuchi, Y.; Watanabe, H. Effective value of the dynamic dilution exponent in bidisperse linear polymers: From 1 to 4/3. *Macromolecules* **2012**, *45* (4), 2085−2098.
(35) Colby, R. H.; Rubinstein, M. Two-parameter scaling for polymers in θ solvents. *Macromolecules* **1990**, *23* (10), 2753−2757.
(36) Shahsavan, F. *Chain dynamics in complex polymer architectures probed by rheology and NMR*; Dissertation, Martin Luther University Halle-Wittenberg: Halle, 2023.
(37) Ahmadi, M.; Bailly, C.; Keunings, R.; Nekoomanesh, M.; Arabi, H.; van Ruymbeke, E. Time marching algorithm for predicting the linear rheology of monodisperse comb polymer melts. *Macromolecules* **2011**, *44* (3), 647−659.
(38) van Ruymbeke, E.; Keunings, R.; Bailly, C. Prediction of linear viscoelastic properties for polydisperse mixtures of entangled star and linear polymers: Modified tube-based model and comparison with experimental results. *J. Non-Newtonian Fluid Mech.* **2005**, *128* (1), 7−22.
(39) Snijkers, F.; Pasquino, R.; Olmsted, P. D.; Vlassopoulos, D. Perspectives on the viscoelasticity and flow behavior of entangled linear and branched polymers. *J. Phys.: Condens. Matter* **2015**, *27* (47), No. 473002.
(40) Anderson, P.-W.; Weiss, P. R. Exchange narrowing in paramagnetic resonance. *Rev. Mod. Phys.* **1953**, *25* (1), 269.
(41) Ball, R. C.; Callaghan, P. T.; Samulski, E. T. A simplified approach to the interpretation of nuclear spin correlations in entangled polymeric liquids. *J. Chem. Phys.* **1997**, *106* (17), 7352−7361.
(42) Saalwächter, K. ^{1}H multiple-quantum nuclear magnetic resonance investigations of molecular order in polymer networks. II. Intensity decay and restricted slow dynamics. *J. Chem. Phys.* **2004**, *120* (1), 454−464.
(43) Baum, J.; Pines, A. NMR studies of clustering in solids. *J. Am. Chem. Soc.* **1986**, *108* (24), 7447−7454.
(44) Kresse, B.; Hofmann, M.; Privalov, Af; Fatkullin, N.; Fujara, F.; Rössler, E. A. All polymer diffusion regimes covered by combining field-cycling and field-gradient 1H NMR. *Macromolecules* **2015**, *48* (13), 4491−4502.
(45) Lozovoi, A.; Mattea, C.; Hofmann, M.; Saalwaechter, K.; Fatkullin, N.; Stapf, S. Segmental dynamics of polyethylene-alt-propylene studied by NMR spin echo techniques. *J. Chem. Phys.* **2017**, *146* (22), 224901.
(46) Mordvinkin, A.; Saalwächter, K. Microscopic observation of the segmental orientation autocorrelation function for entangled and constrained polymer chains. *J. Chem. Phys.* **2017**, *146* (9), 94902.
(47) Kimmich, R.; Köpf, M.; Callaghan, P. Components of transverse NMR relaxation in polymer melts: Influence of chain-end dynamics. *J. Polym. Sci., Part B: Polym. Phys.* **1991**, *29* (8), 1025−1030.
(48) Schillé, E.; Cohen Addad, J.-P.; Guillermo, A. Concentrated solutions of partly deuterated triblock polybutadiene Segmental analysis of NMR properties. *Macromolecules* **2004**, *37* (6), 2144−2150.
(49) Keller, J. *Molecular relaxation of partially deuterated polyisoprene model melts studied by rheology and $^{1}H/^{2}H$ time domain NMR*; Dissertation, Karlsruher Institut für Technologie (KIT): Karlsruhe, 2021, *2021*.

https://doi.org/10.1021/acs.macromol.4c02015
Macromolecules 2024, 57, 11030−11041